JOURNAL OF VIROLOGY, Jan. 1997, p. 548–561 Vol. 71, No. 1
0022-538X/97/$04.00+0

The Early Region 1B 55-Kilodalton Oncoprotein of Adenovirus Relieves Growth Restrictions Imposed on Viral Replication by the Cell Cycle

FELICIA D. GOODRUM[1] AND DAVID A. ORNELLES[1,2]*

Molecular Genetics Program[1] and Department of Microbiology and Immunology,[2] Bowman Gray School of Medicine, Wake Forest University, Winston-Salem, North Carolina 27157-1064

Received 23 July 1996/Accepted 20 September 1996

The E1B 55-kDa oncoprotein of adenovirus enables the virus to overcome restrictions imposed on viral replication by the cell cycle. Approximately 20% of HeLa cells infected with an E1B 55-kDa mutant adenovirus produced virus when evaluated by electron microscopy or by assays for infectious centers. By contrast, all HeLa cells infected with a wild-type adenovirus produced virus. The yield of E1B mutant virus from randomly cycling HeLa cells correlated with the fraction of cells in S phase at the time of infection. In synchronously growing HeLa cells, approximately 75% of the cells infected during S phase with the E1B mutant virus produced virus, whereas only 10% of the cells infected during G_1 produced virus. The yield of E1B mutant virus from HeLa cells infected during S phase was sevenfold greater than that of cells infected during G_1 and threefold greater than that of cells infected during asynchronous growth. Cells infected during S phase with the E1B mutant virus exhibited severe cytopathic effects, whereas cells infected with the E1B mutant virus during G_1 exhibited a mild cytopathic effect. Viral DNA synthesis appeared independent of the cell cycle because equivalent amounts of viral DNA were synthesized in cells infected with either wild-type or E1B mutant virus. The inability of the E1B mutant virus to replicate was not mediated by the status of p53. These results define a novel property of the large tumor antigen of adenovirus in relieving growth restrictions imposed on viral replication by the cell cycle.

Adenovirus (Ad) encodes proteins that deregulate normal cellular growth to the advantage of viral replication (reviewed in references 7 and 67). The oncoproteins of Ad are encoded within the early regions 1A (the E1A 12S and 13S proteins) and 1B (the E1B 55-kDa and 19-kDa proteins). The E1A proteins have been shown to deregulate the cell cycle and induce cellular DNA synthesis by binding cellular regulatory proteins such as pRb and p300 (reviewed in reference 17). Less is known about the function of the large tumor antigen of Ad, the E1B 55-kDa protein, during the lytic infection and during cellular transformation or how these functions are linked (61, 69).

During the late stage of a lytic infection, the E1B 55-kDa protein, in complex with the E4 34-kDa protein, preferentially facilitates the transport of viral mRNA while impeding the transport of cellular mRNA (4, 8, 23, 36, 45). Consequently, Ad mutants that fail to express the E1B 55-kDa protein are defective for expression of viral late proteins. The defect in mRNA transport lies at an intranuclear step after mRNA synthesis but before translocation through the nuclear pore complex (36, 45). The E1B 55-kDa protein has also been demonstrated to directly inhibit host protein synthesis by mechanisms unrelated to the inhibition of mRNA transport (3).

Alone, the E1B 55-kDa protein has no transforming activity (64). However, the E1B 55-kDa and E1B 19-kDa proteins cooperate with the E1A proteins to fully transform nonpermissive cells (6, 18, 20, 54). The E1B 55-kDa protein contributes to transformation by inactivating the cellular tumor suppressor p53 (73). This inhibition of p53-mediated transactivation is required for transformation by both the weakly oncogenic group C and highly oncogenic group A Ad (30, 72, 74, 75). In addition, the E1B gene products have been shown to cooperate with E1A proteins to down regulate p53-driven expression of cyclin D1, which is required for cells to progress through the G_1 phase of the cell cycle (60). Also in cooperation with E1A proteins, the E1B 55-kDa protein stimulates cellular DNA synthesis in nonpermissive cells (50). Thus, in cooperation with other viral proteins, the E1B 55-kDa protein appears to promote a favorable cellular environment for the transformation of nonpermissive cells.

A potential role for the E1B 55-kDa protein in deregulating the cell cycle during the lytic infection has been examined in the work presented here. Ad mutants that fail to express the E1B 55-kDa protein replicated poorly, producing approximately 35-fold fewer progeny virions than a wild-type virus. Although each HeLa cell was infected, only 20% of the cells in an infected population produced progeny E1B mutant virus. However, as many as 75% of the HeLa cells infected with the E1B 55-kDa mutant virus during S phase produced virus, whereas only 10% of cells infected with the same virus during G_1 produced virus. Cell populations infected during S phase also produced higher titers of the E1B 55-kDa mutant virus than cells infected during G_1. These results suggest that the E1B 55-kDa protein functions directly in overcoming the growth restrictions imposed on viral replication by the cell cycle.

MATERIALS AND METHODS

Cell culture. Cell culture media, cell culture supplements, and serum were obtained from Life Technologies (Gibco/BRL, Gaithersburg, Md.) through the Tissue Culture Core Laboratory of the Comprehensive Cancer Center of Wake Forest University. HeLa (ATCC CCL 2, Rockville, Md.), A549 (ATCC CCL 185), and 293 (ATCC CRL 1573) cells were maintained as monolayers in Dulbecco-modified Eagle's minimal essential medium (DMEM) supplemented with 10% newborn calf serum (CS), 100 U of penicillin, and 100 μg of streptomycin per ml. Saos-2 (ATCC HTB 85) cells were maintained as monolayers in DMEM supplemented with 5% fetal bovine serum (FBS), 100 U of penicillin, and 100 μg

* Corresponding author. Mailing address: Department of Microbiology and Immunology, Bowman Gray School of Medicine of Wake Forest University, Winston-Salem, NC 27157-1064. Phone: (910) 716-9332. Fax: (910) 716-9928. E-mail: ornelles@mgrp.bgsm.edu.

of streptomycin per ml. NCI-H460 (ATCC HTB 117) and NCI-H358 (ATCC CTL 5807) were purchased from the American Type Culture Collection (Rockville, Md.) and maintained in antibiotic-free RPMI 1640 supplemented with 10% FBS and essential amino acids. Cells were maintained in subconfluent adherent cultures in a 5% CO_2 atmosphere at 37°C by passing twice weekly at a 1:10 dilution. Cells were preserved in liquid nitrogen in 93% FBS and 7% dimethyl sulfoxide.

Synchronization of the HeLa cell cycle was achieved by a combination of mitotic detachment and hydroxyurea block modified from previously described methods (11). HeLa cells were passaged 1:5 into 75-cm^2 flasks for synchronization 16 to 24 h prior to the mitotic detachment. All but 5 ml of growth media was removed, and the flasks were tapped sharply five times on each of the three flat sides. The detached cells were resuspended in DMEM + 10% CS + 2 mM hydroxyurea (Sigma, St. Louis, Mo.), replated at 2×10^5 cells per ml, and incubated at 37°C in a 5% CO_2 atmosphere. After 1 h, the medium and nonadherent cells were replaced with fresh DMEM + 10% CS + 2 mM hydroxyurea and incubated for 11 h at 37°C in a 5% CO_2 atmosphere. At the completion of the incubation with hydroxyurea, the cells were washed twice with warm phosphate-buffered saline (PBS) (137 mM NaCl, 3 mM KCl, 1.76 mM KH_2PO_4, 10 mM $NaHPO_4$) and the last wash was replaced with normal growth medium to release the G1/S block.

Viruses. The phenotypically wild-type Ad type 5, *dl*309 (26), used in these studies served as the parent virus to the mutant viruses containing a large deletion in the gene encoding the E1B 55-kDa protein, *dl*338 (45), or the E1B 19-kDa protein, *dl*337 (44). The E1B 55-kDa mutant virus, *dl*1520D, has been described previously (6). The propagation of these viruses has been described elsewhere (26). In brief, virus stocks were prepared by infecting 293 cells at a multiplicity of infection of 1 to 3. Virus was harvested 3 days after infection from a concentrated freeze-thaw lysate by sequential centrifugation in discontinuous and equilibrium cesium chloride gradients (25). The gradient-purified virus was supplemented with 5 volumes of 12 mM HEPES (pH 7.4), 120 mM NaCl, 0.1 mg of bovine serum albumin (fraction V; Life Technologies Inc.) per ml, 50% glycerol (Fisher Scientific, Pittsburgh, Pa.) and stored at −20°C. The titers of *dl*309 (8×10^9 PFU per ml) and *dl*338 (2.5×10^9 PFU per ml) were determined by plaque assays using 293 cells as previously described (25).

For infection with Ad, cells were passaged 16 to 24 h prior to infection to achieve approximately 40% confluence at the time of infection. Cells were washed twice with PBS, and the final wash was replaced with virus (5 to 10 PFU per cell) in Ad infection medium (PBS supplemented with 0.2 mM $CaCl_2$, 0.2 mM $MgCl_2$, 2% CS, 100 U of penicillin, and 100 μg of streptomycin per ml). The virus was added at one-fourth the normal culture volume, and the cells were gently rocked for 60 to 90 min at 37°C. The virus suspension was then replaced with normal growth medium, and the infected cells were returned to 37°C.

Electron microscopy. HeLa cells were fixed for transmission electron microscopy with 2.5% glutaraldehyde in PBS + 1.5 mM $MgCl_2$ at 20 h postinfection. The fixed cell pellet was postfixed with osmium tetroxide in phosphate buffer and dehydrated in a graded series in alcohol. Specimens were infiltrated with Spurr's resin-propylene oxide and cut into approximately 100-nm-thick sections with a diamond knife. Sections were collected on copper grids and stained with uranyl acetate and lead citrate and analyzed at 80 keV with a Philips 400 transmission electron microscope. Specimens were embedded and sectioned by MicroMed, the Electron Microscopy Core Laboratory of the Comprehensive Cancer Center of Wake Forest University.

Indirect immunofluorescence. Indirect immunofluorescence and photomicroscopy of whole cells was performed as described previously (43). For staining the Ad E2A 72-kDa DNA-binding protein, the E2A 72-kDa-specific monoclonal antibody (clone B6-8) (51) was used as hybridoma cell medium diluted 1:2 in Tris-buffered saline (137 mM NaCl, 3 mM KCl, 25 mM Tris-Cl [pH 8.0], 1.5 mM $MgCl_2$, 0.5% bovine serum albumin, 0.1% glycine, 0.05% Tween 20, 0.02% sodium azide). The primary antibody was visualized with fluorescein-conjugated goat antibodies specific for mouse immunoglobulin G (Jackson Immunoresearch, West Grove, Pa.). Cells were examined and photographed by epifluorescence with a Leitz Dialux 20 EB microscope.

Plaque assay for infectious centers. The percentage of cells producing virus was determined by a modified plaque assay for infectious centers (34, 58). Either asynchronous or synchronized HeLa cells were passed to 2×10^5 cells per ml 16 to 24 h prior to infection. HeLa cells were infected with 5 to 10 PFU per cell of either the wild-type (*dl*309) or the E1B 55-kDa mutant (*dl*338) virus. The infected cells were incubated with virus for 2 h at 37°C to allow viral attachment and penetration. The virus was removed, and cells were washed twice with PBS. The cells were collected, and the extracellular virus was inactivated by incubation with 0.25% trypsin-EDTA for 10 min at 37°C. The trypsin was neutralized with DMEM + 10% CS. The infected cells were diluted to various cell densities (4,000, 2,000, 1,000, 500, and 250 cells per ml) in DMEM + 10% CS, and 0.1 ml of each cell dilution was added to 0.1 ml of 2.8% agarose type VII (Sigma) in DMEM with 0.6% sodium bicarbonate at 42°C. The cells were gently overlaid onto subconfluent 293 cells plated in 65-mm-diameter dishes. Once the initial agar overlay solidified, cells were overlaid with 0.7% SeaKem ME agarose (FMC, Rockland, Maine) in DMEM with 0.75% sodium bicarbonate and 4% CS. The infected cells were scored as plaques by staining with neutral red on day 9 after infection. The data were analyzed by plotting the number of infectious centers (plaques) obtained versus the number of infected cells plated.

$TCID_{50}$ assay for infectious centers. The percentage of HeLa cells producing virus was statistically determined from a modification of the 50% tissue culture infectious dose ($TCID_{50}$) assay (15). Asynchronous or synchronized HeLa cells were passaged, infected, and harvested 2 h postinfection as previously described for the plaque assay for infectious centers. The infected cells were diluted in growth medium to 1,000, 250, 64, 16, 4, 1, and 0.24 cells per ml, and mock-infected HeLa cells were diluted to 1,000 cells per ml. One-tenth milliliter of each dilution was added to each of 12 wells of a 96-well culture dish, and the infected HeLa cell culture was returned to growth conditions. At 48 h postinfection, the infected HeLa cells were lysed in the 96-well dish by freezing and thawing three times. The entire HeLa cell lysate containing any released progeny virus was transferred onto subconfluent monolayers of 293 cells grown in a 96-well dish. The plate was scored for infected wells 5 days later by evaluating the 293 cell monolayer at low power through an inverted microscope for cytopathic effect. The fraction of infected wells was expressed as a function of the number of infected HeLa cells added to each well, and the data were fit to equation 1:

$$f = \frac{1}{1 + (a/n)^b}$$

where f is the fraction of infected wells and n is the number of cells added per well. The parameters a and b were determined by the method of nonlinear, least squares analysis using MacCurvefit (Kevin Raner Software, Waverley, Australia). When b is fixed at 1, a is the $TCID_{50}$. By assuming a Poisson distribution for the number of infected cells and setting $b = 1$, the number of cells required to obtain an infectious center (virus-producing cell) was determined by solving equation 1 for n when $f = 1/e = 0.632$. The error associated with b after b was forced to 1 was typically ±0.15 and did not exceed ±0.35 for any values presented in Table 1.

Flow cytometry. HeLa cells were detached with trypsin and fixed in 70% ethanol for 1 h to overnight. The ethanol was removed, and the cells were resuspended to approximately 10^6 cells per ml in propidium iodide buffer (100 mM NaCl, 36 mM sodium citrate, 50 μg of propidium iodide per ml, 0.6% Nonidet P-40) supplemented with 0.04 mg of RNase (Sigma) per ml and Nonidet P-40. The cells were filtered through nylon mesh and passed through a 27.5-gauge needle to achieve a single-cell suspension. The DNA content of individual cells was measured by fluorescence-activated cell sorting (FACS) using a Coulter Epics XL flow cytometer (Coulter Corp, Miami, Fla.) with an argon laser as the excitement source (488 nm). The emitted light was analyzed for forward and 90° scatter, pulse width (to discriminate doublets), and red fluorescence (>630 nM) of propidium iodide to determine the DNA content per nucleus. In most cases, 40,000 events were measured in each analysis. The resulting data were acquired in list mode for discriminatory analysis such as the use of standard gating procedures to define distinct populations of cells, doublets, and debris. All flow cytometric analyses were conducted by the Steroid Receptor Laboratory in cooperation with the Hematology Flow Cytometry Laboratory of North Carolina Baptist Hospital.

Plaque assays. Detailed methods for Ad plaque assays have been described elsewhere (25). In brief, virus was harvested from HeLa cells in culture medium 48 to 72 h postinfection by multiple cycles of freezing and thawing. The cell lysates were clarified by centrifugation and serially diluted in infection medium for infection of 293 cells for plaque assays. After incubation with lysates for 1 h, the 293 cells were overlaid with 0.7% SeaKem ME agarose (FMC) in DMEM supplemented with 0.75% sodium bicarbonate and 4% CS. The cells were fed with additional overlays every third day for 7 days. The plaques were visualized by staining with neutral red in an agarose overlay.

DNA slot blot. The DNA slot blotting procedure has been described previously (2, 29) and is briefly described here. Total cellular DNA was isolated from infected HeLa cells. HeLa cells were collected, pelleted, and resuspended in 10 mM Tris, pH 8.0. An equal volume of lysis buffer was added (400 mM Tris-HCl [pH 8.0], 100 mM EDTA, 1% sodium dodecyl sulfate, and 200 μg of proteinase K per ml), and the cells were kept at 50°C for 1 h. DNA was extracted with phenol-chloroform, precipitated, and quantified by spectrophotometry (A_{260}). Equivalent amounts of total cellular DNA were blotted onto Nytran nylon membranes (Schleicher & Schuell, Inc., Keene, N.H.) using a manifold device (Life Technologies, Gaithersburg, Md.) and vacuum. The immobilized DNA was denatured, neutralized, and cross-linked to the matrix with UV light (Stratalinker; Stratgene, La Jolla, Calif.). The DNA was then hybridized with an excess of [α-^{32}P]dATP-labeled (ICN, Costa Mesa, Calif.) DNA probe generated by random-primed synthesis of wild-type Ad DNA (2). Hybridized probe was quantified with the use of a Molecular Dynamics PhosphorImager and ImageQuant analysis software (Molecular Dynamics, Sunnyvale, Calif.).

RESULTS

The E1B 55-kDa mutant Ad produces virions in a subpopulation of infected HeLa cells. Previous work demonstrated that HeLa cells infected with the E1B 55-kDa mutant Ad *dl*338 produce nearly 2 orders of magnitude fewer progeny virus than cells infected with the wild-type Ad, *dl*309 (45). However, not

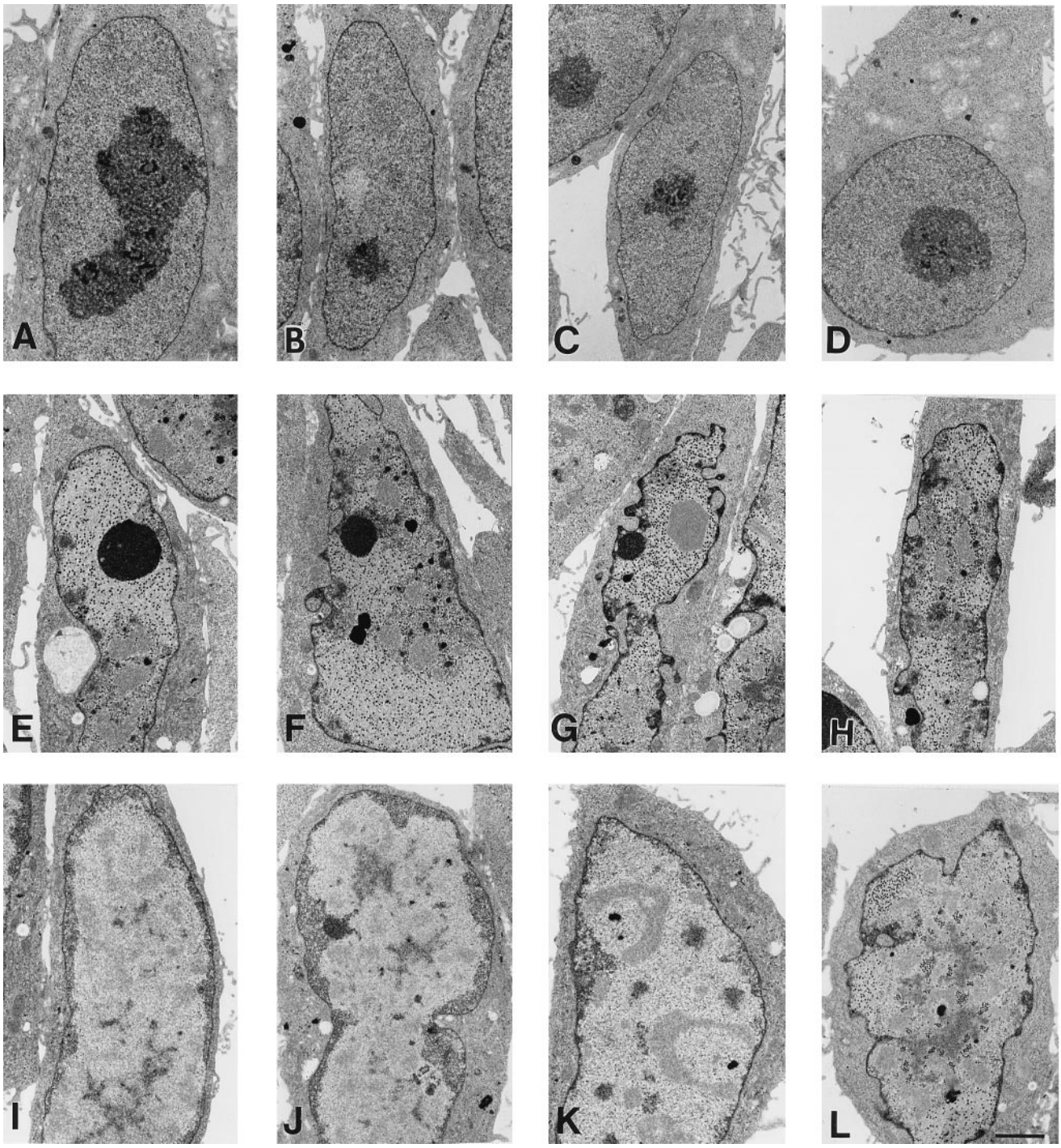

FIG. 1. Only 20% of HeLa cells infected with an E1B 55-kDa mutant virus contain viral particles, whereas all cells infected with a wild-type virus contain viral particles. Monolayers of HeLa cell were mock infected (A to D) or infected with either the wild-type virus, *dl*309 (E to H), or the E1B 55-kDa mutant virus, *dl*338 (I to L), at a multiplicity of 10 PFU per cell. At 20 h postinfection, cells were fixed in 2.5% glutaraldehyde, embedded, and sectioned for transmission electron microscopy. Nearly all (>97%) cells infected with wild-type virus contained electron-dense viral particles in the nucleus by 20 h postinfection. Four representative wild-type virus-infected cells are shown in panels E through H. Of the four representative cells infected with the E1B mutant virus (I to L), only the cell in panel L displays viral particles in the nucleus. All cells shown are representative of each infected population. Bar, 2 μm.

all cells infected with the E1B 55-kDa mutant virus contained progeny viral particles when evaluated by electron microscopy, as shown in Fig. 1. HeLa cells were mock infected or infected with either wild-type or E1B 55-kDa mutant Ad and processed for transmission electron microscopy 20 h after infection. The nuclear structures evident in the mock-infected cells seen in Fig. 1A to D include the nucleolus, cellular chromatin, and granules of chromatin or ribonucleoprotein. In cells infected with wild-type virus, the nuclear membrane has become crenulated, the nucleolus has changed in appearance, and cellular

chromatin has condensed at the periphery of the nucleus. In addition, virus-specific inclusions and virus particles were evident in the nuclei of nearly all cells infected with the wild-type virus (Fig. 1E to H). At the magnification of Fig. 1, the virus particles appear as small, densely stained particles. At higher magnification, the Ad particles are icosahedral in symmetry and are uniform in size and shape (Fig. 2B, inset).

Strikingly, the majority of cells infected with the E1B 55-kDa mutant virus failed to produce any intranuclear viral particles, although all cells contained the characteristic viral nuclear inclusions and displayed crenulated nuclear membranes (Fig. 1I to L). In more than 400 infected cells evaluated by transmission electron microscopy, approximately 20% of the E1B mutant virus-infected population contained virus. Of the four representative cells infected with the E1B 55-kDa mutant virus in Fig. 1I to L, only the cell in panel L contained progeny virus particles. In addition, those E1B 55-kDa mutant virus-infected cells that contained progeny virus particles appeared to contain fewer progeny virions than any wild-type-infected cell examined. Thus, although 20% of the population of E1B mutant virus-infected cells appeared to permit replication of the mutant virus, these cells produced less than a wild-type yield of virus. This result is to be expected because if 20% of the cells (1 in 5) produced E1B mutant virus, each cell would have to produce approximately 20-fold fewer virus particles than those seen in a wild-type virus-infected cell to account for the 100-fold reduced yield compared with cells infected with the wild-type virus.

The cells in Fig. 1K and L, are shown at higher magnification in Fig. 2A and B, respectively. The cell shown in Fig. 2A failed to produce intracellular virus and represents approximately 80% of the E1B 55-kDa mutant virus-infected cell population. The cell seen in Fig. 2B contains intracellular virus that can be seen in the enlarged inset of a representative region of the nucleus. This cell is typical of 20% of the HeLa cells infected with the E1B mutant virus. Except for the paucity of virus particles in the nucleus, the ultrastructural morphology of cells infected with the E1B 55-kDa mutant virus was similar to that of cells infected with the wild-type virus.

Among cells infected with either the E1B 55-kDa mutant or the wild-type virus, all cells appeared to be infected as determined by electron microscopy. During the late phase of infection, the nucleus becomes occupied by clear fibrillar inclusions, referred to here as viral inclusions (Fig. 2, VI). The viral inclusions seen in the electron micrographs indicated a successful infection by either the wild-type or E1B 55-kDa mutant Ad infection. These inclusions were apparent in all infected cells that were examined and can be recognized in the low magnification images of Fig. 1E to L. Mock-infected cell nuclei were devoid of structures resembling viral inclusions (Fig. 1A to D). Viral inclusions have been shown to be the centers of viral DNA synthesis and accumulation (9, 38, 40, 47, 48, 66) and late viral RNA synthesis and processing (38, 40, 46, 49, 70).

An alternative assay using indirect immunofluorescent staining for the Ad E2A 72-kDa DNA-binding protein confirmed that essentially all cells (>99%) were infected with either wild-type or E1B 55-kDa mutant virus under the conditions used in this study. HeLa cells were infected with either the wild-type or the E1B 55-kDa mutant virus at 10 PFU per cell and processed for indirect immunofluorescence at 14 h postinfection. Cell nuclei were visualized by staining with 4,6-diamidino-2-phenylindole (DAPI, Sigma) a nonspecific DNA-binding stain (Fig. 3A and C). The cells were also stained with a monoclonal antibody (B6-8) against the Ad DNA-binding protein that localizes to the viral inclusions late in infection (51). Viral inclusions were visualized as discrete points of fluorescence in the infected cell nucleus. The representative fields of wild-type virus- and E1B mutant virus-infected cells shown in Fig. 3 demonstrate that all cells were infected (compare Fig. 3A with B and C with D). Taken together, the electron microscopic and immunofluorescent analysis indicated that all cells were infected, although not all cells in the E1B 55-kDa mutant virus-infected populations contained intracellular virus.

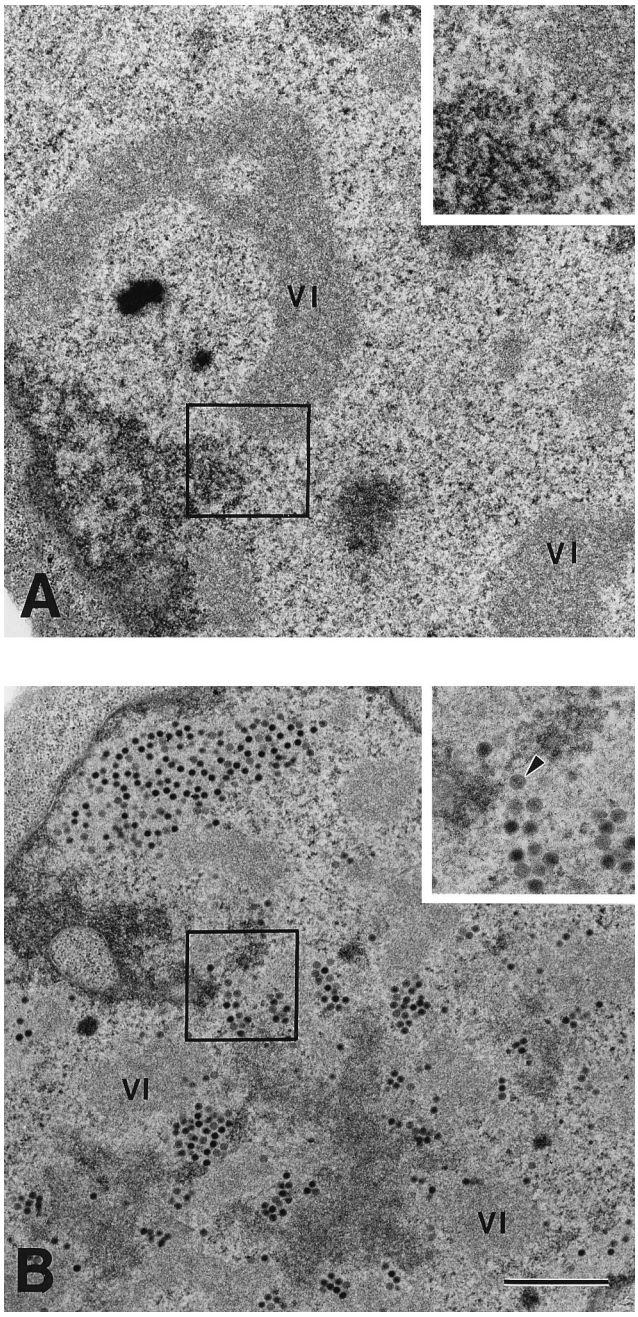

FIG. 2. The E1B 55-kDa mutant virus appears to replicate in only 20% of the infected HeLa cells. The E1B 55-kDa mutant virus-infected cells in panels K and L of Fig. 1 are shown at higher magnification in panels A and B of this figure, respectively. The cell in panel A is representative of approximately 80% of the cells in an E1B 55-kDa mutant virus-infected population. The cell in panel B is representative of 20% of the E1B 55-kDa mutant virus-infected cells. The insets are threefold enlargements of the boxed regions of the nucleus. Adenovirus particles are clearly evident (arrowhead) in the enlarged inset of panel B, whereas no virus particles are apparent in panel A. The presence of viral inclusions (VI) in nearly all cells examined indicates that all cells were infected. Bar, 1 μm.

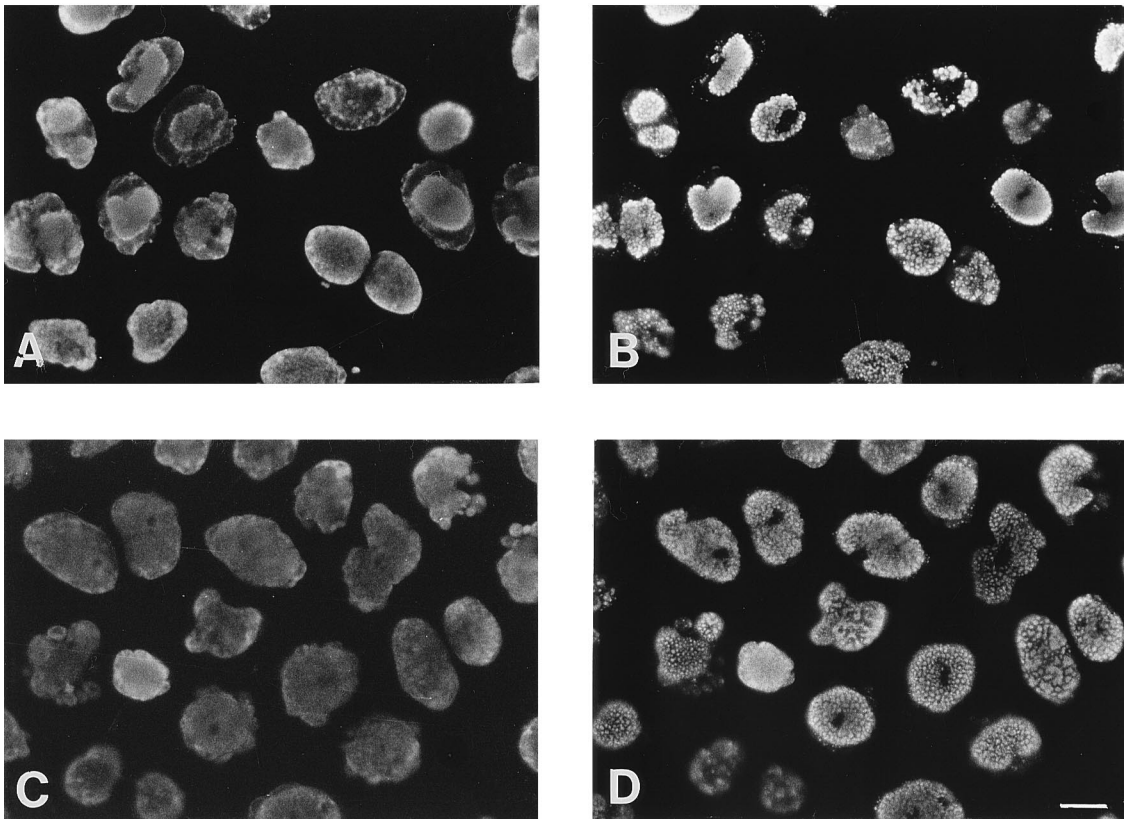

FIG. 3. All cells infected with the wild-type or E1B 55-kDa mutant virus are infected, as determined by an immunofluorescent assay for the E2A DNA-binding protein. HeLa cells were infected with either the wild-type virus, *dl*309, or the E1B 55-kDa mutant virus, *dl*338, at a multiplicity of 10 PFU per cell. The cells were processed for indirect immunofluorescence at 16 h postinfection. All cells in the field are visualized by DAPI staining as seen in panels A and C. The E2A 72-kDa DNA-binding protein was visualized by indirect immunofluorescence in cells infected with the wild-type virus in panel B and in cells infected with the E1B 55-kDa mutant virus in panel D. Typically, greater than 99% of the cells visualized with DAPI also demonstrated DNA-binding protein-specific fluorescence. Bar, 20 μm.

The failure of the cells infected with *dl*338 to produce virus in most infected cells is a property shared by another E1B 55-kDa mutant virus, *dl*1520. The large deletion and premature termination codon in the E1B 55-kDa coding region of *dl*1520 precludes expression of any E1B 55-kDa-related protein (6), whereas the deletion present in the *dl*338 genome could allow expression of a truncated (17-kDa) E1B 55-kDa protein. HeLa cells were infected with the E1B 55-kDa mutant virus, *dl*1520D, or the E1B 19-kDa mutant virus, *dl*337, at 10 PFU per cell. At 20 h postinfection, the infected cells were processed for transmission electron microscopy. In an identical manner to HeLa cells infected with *dl*338, only 20% of the cells infected with *dl*1520 produced progeny virions (data not shown). By contrast, all cells infected with the E1B 19-kDa mutant virus, *dl*337, produced progeny virus (data not shown). These results suggest that the inability to replicate in all infected cells is a property of viruses containing mutations that specifically inactivate or delete the E1B 55-kDa coding region and is not common to all mutations within the early region 1B.

The results obtained by electron microscopy suggest that only 20% of the HeLa cells infected with the E1B 55-kDa mutant virus produce particles that appear to be progeny virions. These morphological data were confirmed by a plaque assay modified to measure virus-producing cells or infectious centers. For this assay, HeLa cells were infected with either the wild-type or the E1B 55-kDa mutant virus at 10 PFU per cell for 90 min. The extracellular virus was inactivated by incubating the cells with a mixture of trypsin and EDTA for 10 min. Various numbers of infected HeLa cells in molten agar were overlaid onto a monolayer of 293 cells. 293 cells express the early region 1 products of Ad5 and are permissive for the replication of all Ad E1 mutants (21). Plaques were formed when an infected HeLa cell in the agar overlay successfully replicated the virus and lysed and infected 293 cells below the agar overlay. The number of plaques obtained was plotted on the abscissa as a function of the number of infected cells plated. In the representative experiment shown in Fig. 4, the line corresponding to cells infected with the wild-type virus (circles) has a slope of 0.24 ± 0.05 infectious centers per cell, whereas the slope of the line corresponding to cells infected with the E1B mutant virus (squares) is 0.060 ± 0.003. The ratio of these values (0.06/0.24) is 0.25, indicating that cells infected with mutant virus produce infectious centers at 25% of the frequency of cells infected with the wild-type virus. From six independent experiments, an average of $22 \pm 4\%$ of cells infected with the E1B 55-kDa mutant virus produced infectious progeny virus compared to cells infected with the wild-type virus. These results precisely agree with the results obtained by electron microscopy.

Replication of the E1B 55-kDa mutant Ad is dependent on cell density. Because not all HeLa cells in an infected population replicate the E1B 55-kDa mutant virus, it seems likely that differences in the physiological state among individual cells dictate permissivity for replication of an Ad mutant that fails to express the E1B 55-kDa protein. Because the physiological state of the cells, including the specific stage of the cell cycle at

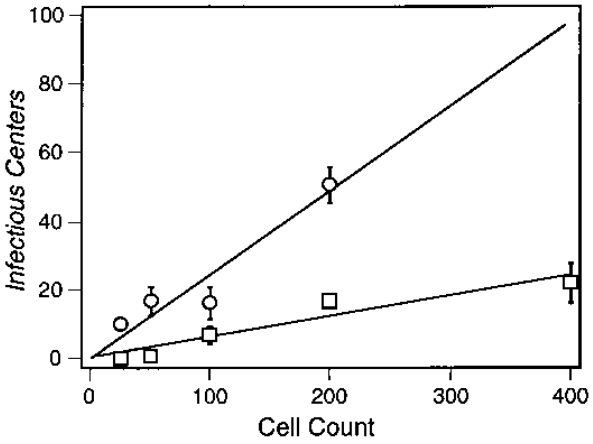

FIG. 4. A plaque assay for infectious centers indicates that fewer HeLa cells infected with the E1B 55-kDa mutant virus replicate the virus than cells infected with the wild-type virus. HeLa cells were infected with either the wild-type virus, *dl*309, or the E1B 55-kDa mutant virus, *dl*338, at a multiplicity of 5 to 10 PFU per cell. The virus was inactivated, and the infected HeLa cells were harvested 90 min postinfection and diluted in molten agar. Various numbers of infected cells in agar were overlaid onto a monolayer of 293 cells. Plaques were formed when an infected HeLa cell in the agar overlay successfully replicated the virus and lysed and infected 293 cells below the agar overlay. The number of plaques obtained was plotted on the abscissa as a function of the number of infected cells plated (ordinate). A representative experiment is shown with results obtained from HeLa cells infected with the wild-type virus (○) and HeLa cells infected with the E1B mutant virus (□). The standard error associated with the dependent variable (infectious centers) is plotted for each datum. The error associated with the value in the ordinate (cell number) was not determined.

the time of infection, is sensitive to cell density, this relationship was systematically investigated (Fig. 5). For this experiment, HeLa cells were plated at various densities prior to infection. The cells were infected with the wild-type or the E1B mutant virus at 10 PFU per cell, and the virus yield was measured by a plaque assay. Identically treated cells were harvested at the time of infection and analyzed by FACS to determine if the cell cycle distribution in the population of cells varied with cell density. The results shown in Fig. 5A demonstrate that wild-type Ad replication is largely independent of cell density. By contrast, the yield of the E1B 55-kDa mutant virus showed an inverse dependence on cell density (Fig. 5B). In two independent experiments, HeLa cells infected at increasing cell densities produced lower yields of E1B mutant virus per cell. Furthermore, as the HeLa cell density increased, the percentage of cells in S phase decreased (Fig. 5C) and the percentage of cells in G_1 increased (not shown). These results agree with previous findings suggesting that as HeLa cells grow to increased density, they partially arrest in G_1 (32, 71). Indirect immunofluorescent staining for the Ad DNA-binding protein demonstrated that the lower virus yields associated with increasing cell density were not the result of decreased infectivity. All cells in each wild-type or mutant virus-infected population expressed the viral DNA-binding protein, irrespective of cell density (data not shown). The dependence of the E1B 55-kDa mutant virus on cell density for replication coupled with the observation that only ≈20% of HeLa cells infected with the E1B 55-kDa mutant virus replicate the virus suggests that, in contrast to the wild-type virus, the E1B 55-kDa mutant virus requires cells to be in S phase for viral replication.

The E1B 55-kDa mutant virus produces virus in a greater percentage of cells infected during S phase than cells infected during G_1. To determine if the stage of the cell cycle at the time of infection impacts replication of the E1B 55-kDa mutant virus, HeLa cells were synchronized and infected at various points throughout the cell cycle. For all experiments using synchronized cells, a parallel set of cells was analyzed by FACS. The DNA content of each cell was measured, and this value was used to determine the stage of the cell cycle for each cell. The results of a typical synchronization procedure are shown in Fig. 6. Asynchronously growing HeLa cells (Fig. 6A) were found to contain 65% cells in G_1 (or G_0), 11% in G_2 or

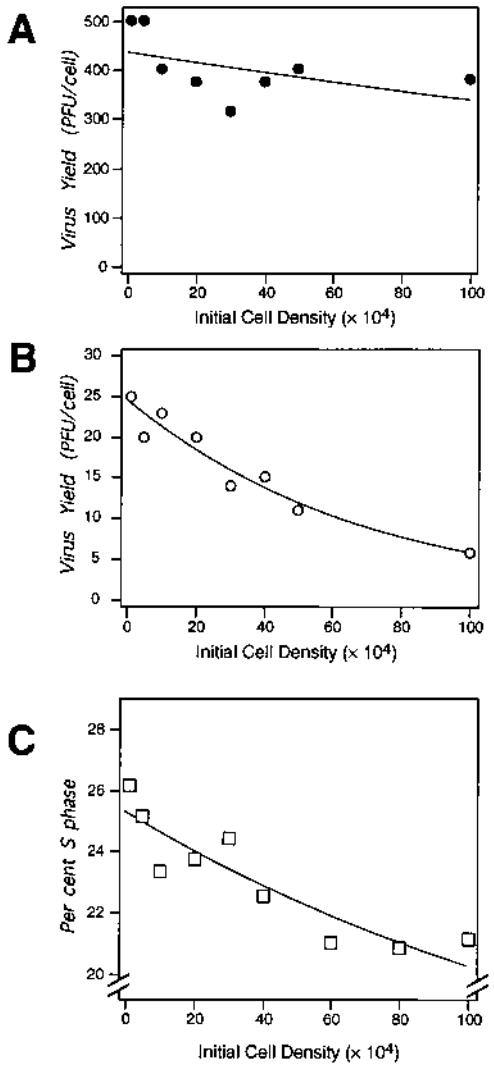

FIG. 5. Replication of the E1B 55-kDa mutant virus depends on cell density. HeLa cells were passed to various cell densities and infected 24 h after attachment with either the wild-type virus, *dl*309, or the E1B 55-kDa mutant virus, *dl*338, at a multiplicity of 10 PFU per cell. Virus yields were measured by plaque assay using 293 cells and are expressed as PFU per cell on the abscissa versus the initial cell density on the ordinate. (A) Replication of the wild-type virus is poorly correlated with the density of the cells at the time of infection (●). The exponential curve shown fits the data with a correlation coefficient of 0.247. The data also fit a horizontal line (not shown) with a correlation coefficient of 0.243. (B) Replication of the E1B 55-kDa mutant virus demonstrated an inverse relationship to cell density (○). The data are shown fit to an exponentially decaying curve with a coefficient of correlation equal to 0.93. (C) The percentage of HeLa cells in S phase was also inversely related to cell density (□). The data in panel C were obtained by plating HeLa cells at the indicated densities and harvesting the cells 24 h after attachment. After staining with propidium iodide, the DNA content of the cells was measured by FACS and used to determine the number of cells in S phase. The data fit an exponentially decaying curve that asymptotically approaches 15%, with a correlation coefficient equal to 0.94.

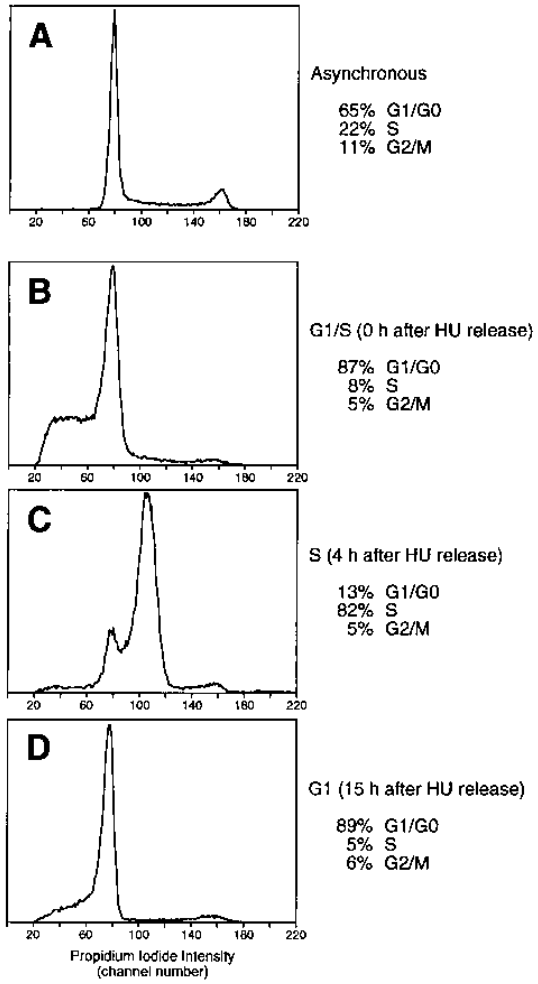

FIG. 6. HeLa cells were synchronized to achieve a high degree of synchrony as determined by FACS analysis. HeLa cells were synchronized by a combination of mitotic detachment and a hydroxyurea block. The hydroxyurea block was released with normal growth medium, and the HeLa cells were allowed to enter S phase synchronously. Asynchronously growing cells as well as synchronized cells obtained 0, 4, and 15 h after release of the hydroxyurea block were fixed and stained with propidium iodide. The intensity of the propidium iodide fluorescence in individual cells was measured by FACS to determine DNA content. The distribution of cells between G_1/G_0, S, and G_2/M phases of the cell cycle was determined by standard means as described in Materials and Methods. The histograms display the number of cells counted at the indicated fluorescence intensity; these values were scaled to accommodate the maximum value for each panel. Typically 40,000 cells were analyzed for each sample. Panel A shows the cell cycle distribution of cells in an asynchronous population. Panel B shows the distribution of cells immediately after the release of the hydroxyurea block in which 87% of the cells occur at the G_1-S boundary. The shoulder in the curve appearing between channel numbers 20 and 68 was infrequently observed in synchronized cell populations. These values most likely are due to dead or apoptotic cells and were not included in the analysis. Panel C shows the synchronous shift of 82% of the HeLa cells into S phase 4 h after release of the hydroxyurea. Panel D shows that 89% of the cells were found in G_1 (or G_0) phase 15 h after hydroxyurea release.

M, and 22% in S phase. HeLa cells were synchronized by a combination of mitotic detachment and hydroxyurea block (11). Hydroxyurea is selectively cytotoxic to cells in S phase and blocks progression through the cell cycle at the G_1/S boundary. Removal of the hydroxyurea block permitted the HeLa cell populations to enter S phase synchronously. An effect of the hydroxyurea treatment can be seen in the histograms of cell number versus DNA content in Fig. 6B. The shoulder preceding the G_1 peak represents cell debris resulting from apoptosis of S phase cells collected by mitotic detachment and treated with hydroxyurea (63). As the synchronized cells progressed through the cell cycle (Fig. 6C and D), this shoulder decreased as apoptotic cells detached from the plates and were washed away. For each experiment a high degree of synchrony was achieved as populations of cells shifted to approximately 87% G_1/S phase (Fig. 6B), 82% S phase (Fig. 6C), or 89% G_1 phase (Fig. 6D).

HeLa cells were synchronized and infected with the wild-type and E1B mutant virus both during early S phase (corresponding to the cells analyzed in Fig. 6B) and during G_1 (corresponding to cells analyzed in Fig. 6D). The infected cells were analyzed by transmission electron microscopy 20 h postinfection. HeLa cells infected with the wild-type virus both during S phase (Fig. 7A) and during G_1 (Fig. 7B) contained progeny viral particles as expected. Viral particles from a representative portion of the nucleus are shown in the insets. No ultrastructural differences were noted between HeLa cells infected with the wild-type virus at S phase or G_1. By contrast, cells infected with the E1B 55-kDa mutant virus during S phase (Fig. 7C) appeared more permissive for replication of the mutant virus than cells infected during G_1 (Fig. 7D) or cells infected as asynchronous populations (Fig. 1 and 2). Greater than 75% of the S phase cells infected with the E1B 55-kDa mutant virus produced intracellular virus particles, as determined by electron microscopy. The percentage of S phase cells that failed to produce mutant virus may be partially accounted for by cells that were not in S phase ($\approx$18%) or were in late S phase at the time of infection due to incomplete synchrony. Only 10% of cells infected with the E1B mutant virus during G_1 produced progeny virus particles (Fig. 7D). The majority of the cells infected with the E1B 55-kDa mutant virus during G_1 were devoid of any particles resembling virions. The small percentage of cells in a G_1 population that produced E1B mutant virions may result from the presence of cells that were in other phases of the cell cycle (S) at the time of infection due to incomplete synchronization. The cells depicted in the micrographs are representative of the majority of each infected population. The presence of viral inclusions in the nuclei of all the cells in each population indicated that all cells were infected (Fig. 7). The results of this electron microscopy study suggest that the replication of an Ad mutant that fails to express the E1B 55-kDa protein depends on a transient environment present in S phase cells at the time of infection.

An endpoint or $TCID_{50}$ assay for infectious centers confirmed that a greater percentage of cells infected with the E1B 55-kDa mutant virus during S phase were permissive for replication of the mutant virus (Table 1) than cells infected in G_1. The $TCID_{50}$ assay for infectious centers was developed for these experiments because the efficiency of detection of infectious centers was greater than that of the plaque assay for infectious centers. HeLa cells infected in an asynchronous state of growth as well as synchronized HeLa cells infected in early S phase or G_1 were compared using this assay. For these experiments, HeLa cells were infected and harvested as for the plaque assay for infectious centers. The infected HeLa cells were replated at various cell numbers (100, 25, 6.4, 1.6, 0.4, 0.1, and 0.024 cells per well) in a 96-well tissue culture dish. After 2 days of incubation to allow virus growth, the infected HeLa cells were lysed in situ to ensure the quantitative release and recovery of progeny virions. The HeLa cell lysates were assayed for the presence of infectious centers by using the lysate to infect a monolayer of 293 cells in a new 96-well tissue culture dish.

The data obtained were fit to equation 1 to determine the

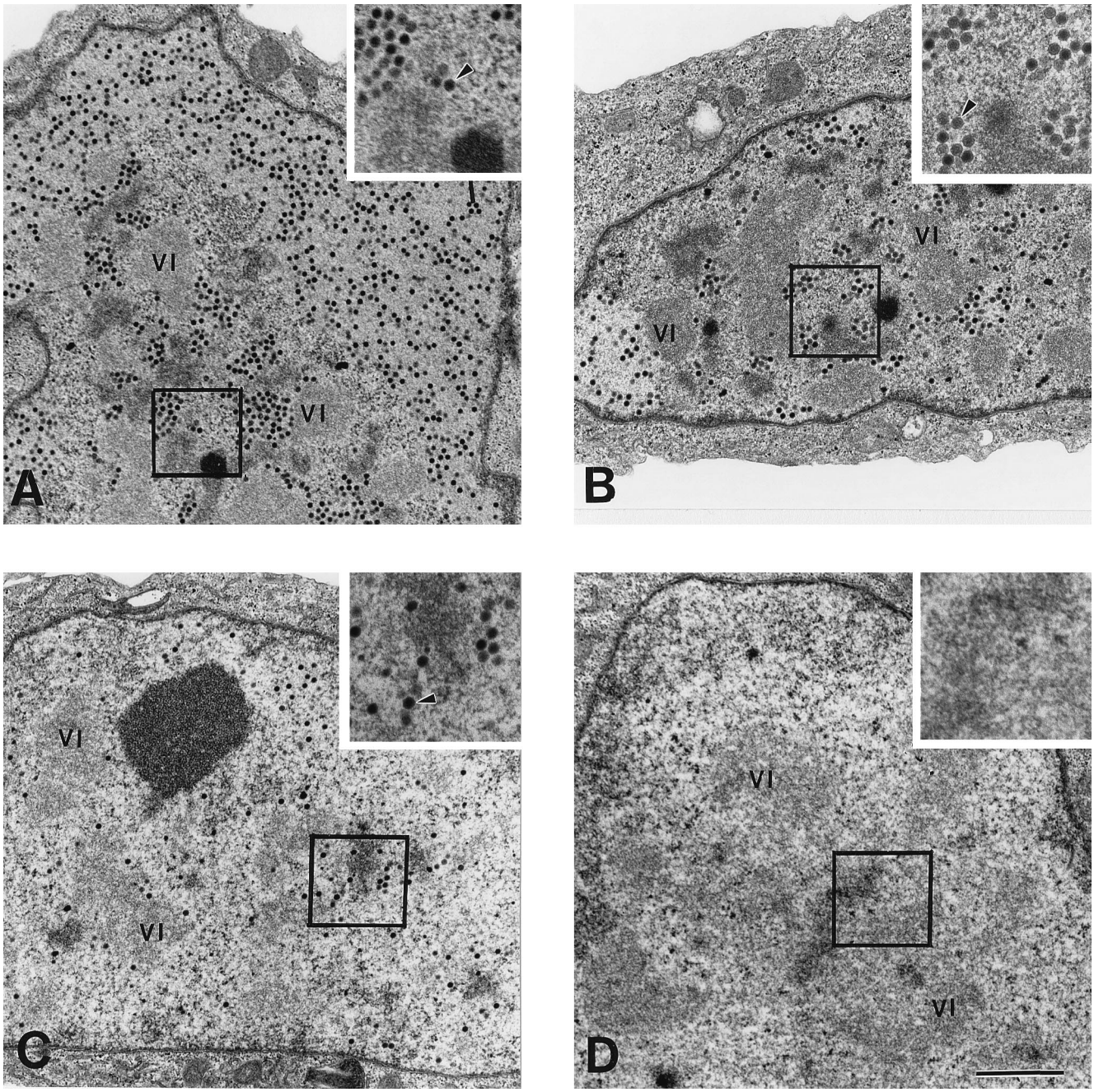

FIG. 7. HeLa cells infected during S phase appear permissive for replication of the E1B 55-kDa mutant virus, whereas cells infected during G_1 do not. HeLa cells were infected at specific points during the cell cycle with either (A and B) the wild-type virus, *dl*309, or (C and D) the E1B 55-kDa mutant virus, *dl*338, at a multiplicity of 10 PFU per cell. The cells in panels A and C were synchronized to S phase at the time of infection. The cells in panels B and D were synchronized to G_1 at the time of infection. At 20 h postinfection, the cells were prepared for transmission electron microscopy. The cells infected with the wild-type virus in panels A and B are representative of the typical wild-type virus-infected cell. The cell seen in panel C is representative of greater than 75% of the cells infected during S phase with the E1B mutant virus. The cell shown in panel D is representative of greater than 85% of the cells infected during G_1 phase with the E1B mutant virus. The insets are threefold enlargements of the boxed regions of the nucleus. Virus particles (arrowheads) are evident in the insets (A, B, and C but not D). All cells were infected as determined by the presence of viral inclusions (VI). Bar, 1 μm.

number of infected cells producing virus. These results indicate that essentially each HeLa cell infected with the wild-type virus was an infectious center regardless of stage of the cell cycle at the time of infection (Table 1). This result is consistent with the results obtained by electron microscopic analysis of HeLa cells infected with the wild-type virus. In addition, this result suggests that the $TCID_{50}$-based assay was more efficient than the plaque-based assay for the detection of infectious centers. The reason for this difference is not known but may be due to inefficient cell lysis and release of progeny virus from cells embedded in the agar in the plaque-based assay. Cells infected during G_1 appeared slightly better able to replicate the wild-type virus compared to a randomly cycling population or S phase population of cells (1 in 0.8 cells versus 1 in 1.4 cells). By

TABLE 1. Infectious centers from asynchronously growing and synchronized HeLa cells infected with wild-type or E1B mutant virus

Virus	Cell cycle[a]	Frequency of infectious centers		
		Replicate values[b]	Avg	Fraction wild type (%)[c]
Wild type	Asynch	1.3 ± 0.2		
		1.6 ± 0.3	1.4 ± 0.15	100 ± 11
		1.1 ± 0.3		
	G_1	0.72 ± 0.1		
		0.85 ± 0.3	0.8 ± 0.12	175 ± 26
		0.80 ± 0.2		
	S	1.2 ± 0.4		
		1.3 ± 0.4	1.4 ± 0.23	100 ± 16
		1.7 ± 0.4		
E1B mutant	Asynch	6.7 ± 1.8		
		5.0 ± 2.5	5.4 ± 1.0	26 ± 5
		4.5 ± 1.0		
	G_1	7.8 ± 2.0		
		8.6 ± 3.8	9.1 ± 1.9	15 ± 3
		10.8 ± 4.1		
	S	4.3 ± 1.5		
		3.2 ± 0.7	3.8 ± 0.65	37 ± 6
		3.9 ± 1.2		

[a] The cells were infected at the stage of the cell cycle indicated. Asynch, cells infected as a randomly cycling population.

[b] The number of cells required to obtain an infectious center ± standard error was determined with the use of equation 1 in three independent replicates.

[c] The fraction of infectious centers (1/number of cells required to obtain an infectious center) ± standard error is expressed as a percentage of the fraction of infectious centers for asynchronously growing cells infected with the wild-type virus.

contrast, only a fraction of the HeLa cells infected with the E1B mutant virus produced virus. Only 1 in 5.4 cells in a randomly cycling population of HeLa cells infected with the E1B mutant virus was productive. Normalized to the number of wild-type virus-infected cells that produce virus (1 in 1.4), this assay would suggest that 26 ± 5% of the E1B mutant-infected cells were productive. This value agrees closely with the value of 20% estimated by electron microscopy (Fig. 1) and the value of 22% estimated by the infectious centers assay by plaque formation (Fig. 4). Also in accord with the electron microscopic analysis, the results in Table 1 reveal that HeLa cells infected in S phase were better able to support replication of the E1B mutant virus than cells infected in G_1. Approximately 2.5-fold more HeLa cells infected in S phase produced the E1B mutant virus than HeLa cells infected in G_1 (1 in 3.8 versus 1 in 9.1). Nonetheless, the normalized fraction of cells infected with the E1B mutant virus during S phase that yielded infectious centers (37 ± 6%) was less than the value of 75% estimated by electron microscopy. The reason for this difference is not understood. Because the infectious centers assay measures infectious virus and electron microscopy visualizes physical particles, it remains possible that some of the cells observed to contain intranuclear viral particles contained non-infectious virions. Finally, the fraction of cells that produced E1B mutant virus after being infected in G_1 (15 ± 3%) is close to the value estimated by electron microscopic analysis. The differences between these two assays could partially be due to variations in the number of non-G_1 cells in the synchronized population arising from incomplete synchronization and a loss of synchrony after progression through one complete cell cycle.

Cells infected during S phase with the E1B 55-kDa mutant virus produce greater yields of progeny virus than do cells infected during G_1. The total yield of virus from cells infected at S and G_1 phase was measured and compared to the yield from asynchronously growing populations of cells. Asynchronous populations of cells infected with the E1B 55-kDa mutant virus produced approximately 35-fold less virus than the wild-type infection (Fig. 8). Infection of synchronized cells with the wild-type virus demonstrated that all cells were permissive for replication of the wild-type virus irrespective of the stage of the cell cycle at the time of infection. However, cells infected with the wild-type virus during G_1 produced threefold more virus than cells infected during S phase. By contrast, the E1B 55-kDa mutant virus replicated most successfully in cells infected during S phase, producing approximately sevenfold more progeny virus than cells infected during G_1 and threefold more virus than asynchronous populations of cells. These results, taken together with the previous infectious center data obtained from synchronized cells, indicate that G_1 cells are better suited for the replication of wild-type virus whereas S phase cells are better suited for the replication of the E1B mutant virus.

Although HeLa cells infected during S phase were better suited for replication of the E1B 55-kDa mutant virus than G_1 cells or asynchronously growing cells, S phase did not entirely complement the defect in viral replication. S phase cells infected with the E1B mutant virus produced ninefold less virus than did wild-type infection. Nonetheless, the data presented thus far indicate that S phase cells are the primary cells permissive for replication of the E1B 55-kDa mutant virus. Ad mutants that fail to express the E1B 55-kDa protein have acquired a dependence on S phase to produce progeny virus. Therefore, the E1B 55-kDa protein appears to overcome restrictions imposed on viral replication by the cell cycle.

HeLa cells infected during different stages of the cell cycle exhibited differing degrees of cytopathic effect, as seen by cell rounding. HeLa cells were infected as an asynchronous population or synchronized and infected in S phase or G_1. The cells were analyzed by phase-contrast microscopy between 24 and 48 h after infection. During this time, mock-infected cells grew

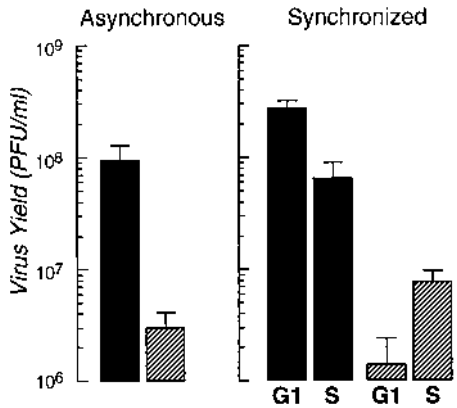

FIG. 8. HeLa cells infected during S phase produce more E1B mutant virus than do asynchronously growing HeLa cells or HeLa cells infected during G_1. Asynchronously and synchronously growing monolayers of HeLa cells were infected with either the wild-type virus, *dl*309, or the E1B 55-kDa mutant virus, *dl*338, at a multiplicity of 10 PFU per cell. The phase of the cell cycle at the time of infection is indicated below the appropriate bar. Cells were lysed 48 h postinfection, and virus yield was measured by plaque assay using 293 cells. The yield (PFU per milliliter) and upper range of the standard error are shown. ■, wild-type virus; ▨, E1B mutant virus.

to confluence and only mitotic cells (<5%) exhibited cell rounding (Fig. 9A). The cytopathic effect induced by the wild-type Ad consisted of severe cell rounding of approximately 70% of the asynchronous infected population by 48 h after infection (Fig. 9B). Asynchronously growing HeLa cells infected with the E1B 55-kDa mutant virus contained approximately 10 to 20% rounded cells (Fig. 9C). All HeLa cells infected with the wild-type Ad during either S phase or G_1 exhibited a cytopathic effect similar to that seen in asynchronous cells (Fig. 9D and F, respectively). However, HeLa cells infected during S phase with the E1B 55-kDa mutant virus showed markedly more severe cytopathic effect than did asynchronous cells or cells infected during G_1 (Fig. 9 compare E with G). Mock-infected synchronized cells exhibited cell rounding only during mitosis at 11 and 33 h after removal of the hydroxyurea block (data not shown). The cell rounding seen in cells infected during either S phase or G_1 was not coincident with the anticipated time of mitosis. This observation indicates that the cell rounding exhibited by cells infected during either S phase or G_1 was due to virus-induced cytopathic effect and not cell division. Although an increased cytopathic effect does not necessarily correlate with virus production, HeLa cells infected in S phase with the E1B 55-kDa mutant virus showed both an increased cytopathic effect and produced more virus than cells infected in G_1. These results lead to the hypothesis that cells infected with the E1B 55-kDa mutant Ad during S phase support an infection that more closely resembles the wild-type virus infection.

Cells infected with the E1B 55-kDa mutant virus synthesize viral DNA to levels of the wild-type virus infection. The failure of G_1 cells to allow replication of the E1B 55-kDa mutant virus could reflect a dependence of the E1B 55-kDa mutant virus on S phase and the cellular program of DNA synthesis in order to synthesize viral DNA. However, the presence of viral centers in the nuclei of all cells in an infected population indicated that viral DNA was synthesized in all cells whether or not they produce progeny virions. In addition, hybridization analysis of total DNA isolated from asynchronous populations of HeLa cells infected with either the wild-type virus or the E1B 55-kDa mutant virus demonstrated that E1B 55-kDa mutant virus-infected cells synthesized viral DNA to levels equivalent to those of wild-type virus-infected cells (Fig. 10). In two independent experiments, the amount of viral DNA synthesized in E1B mutant virus-infected cells either equaled or exceeded the amount of viral DNA synthesized in wild-type virus-infected cells. These data indicate that, in HeLa cells, the E1B 55-kDa mutant virus successfully completes the early phase of viral replication and synthesizes viral DNA to levels equivalent to those of the wild-type infection. Therefore, the lesion of the E1B 55-kDa mutant virus, and presumably the role of the E1B 55-kDa protein, appears to reside in the late phase of viral replication.

The wild-type and E1B 55-kDa mutant viruses not only synthesized equivalent amounts of viral DNA during the course of an infection but also induced the synthesis of viral DNA at the same time in infection. Incorporation of bromodeoxyuridine (BrdU) into mock-infected, wild-type-infected or E1B mutant-infected HeLa cells at various times postinfection demonstrated that both the wild-type virus- and the E1B 55-kDa mutant virus-infected cells induced viral DNA synthesis at approximately 9 h after infection (data not shown). Prior to 9 h after infection, approximately 25 to 30% of both mock-infected and Ad-infected populations of cells incorporated BrdU. By 9 h after infection, 85 to 90% of the cells in both wild-type-infected and E1B 55-kDa mutant virus-infected cultures stained positively for incorporation of BrdU. These results indicate that both the wild-type and E1B mutant Ad initiate viral DNA synthesis at the same time in infection.

The failure of the E1B 55-kDa mutant virus to replicate in all infected cells is not mediated by p53. The experiments discussed above were conducted with HeLa cells that contain a wild-type p53 gene. Normally, the HeLa p53 protein is inactivated by the human papillomavirus early protein E6 (56, 68). However, Ad infection of HeLa cells has been shown to elevate levels of p53, which could hinder viral replication by inducing a G_1 growth arrest and inhibiting viral DNA synthesis (13, 22). During an Ad infection, the E1B 55-kDa protein binds and inactivates p53 (55, 72, 75). Thus, the failure to inactivate p53 may account for the inability of the E1B 55-kDa mutant virus to replicate in all infected cells. To address this hypothesis, two wild-type p53 cell lines, H460 and A549 (10, 35), and two p53-null cell lines, H358 and Saos-2 (39, 62), were analyzed for the ability to allow replication of the E1B mutant virus. If the failure of the E1B 55-kDa mutant virus to replicate was mediated by p53, we would expect that the mutant virus would replicate to levels approaching those of the wild-type virus in a p53-null cell line and replicate poorly in cells containing a wild-type p53. As can be seen in virus yields in Table 2, this effect was not observed.

The E1B 55-kDa mutant virus replicated to the highest titer in H460 and A549 cells expressing the wild-type p53 protein. In addition, both the greatest (18-fold) and least (1.9-fold) difference between replication of the wild-type and E1B mutant virus was observed in the cell lines reported to contain a wild-type p53 gene. Finally, to within 1 log unit, the wild-type virus replicated to the same extent in all cell lines. These results suggest that although replication of the E1B 55-kDa mutant virus is dependent on the cell type, these differences may not be mediated by p53. Taken with the previous results, these findings suggested that the E1B 55-kDa protein relieves growth restrictions by a p53-independent mechanism, perhaps by interacting with other unidentified cellular growth regulatory proteins.

DISCUSSION

The Ad E1B 55-kDa tumor antigen relieves restrictions imposed on viral growth by the cell cycle. Mutant viruses (*dl*338 and *dl*1520) that failed to express the E1B 55-kDa protein produced progeny virions in only 20% of the infected cells as determined by electron microscopy (Fig. 1 and 2 and data not shown). Similarly, assays for infectious centers showed that only 20 to 25% of the cells infected with the E1B 55-kDa mutant virus allowed replication of the mutant virus compared to 100% of the cells infected with the wild-type virus (Fig. 4 and Table 1). The fraction of cells that support growth of the E1B mutant virus is the same as the fraction of cells in S phase in an asynchronously growing culture of HeLa cells (Fig. 5C). The contribution of the cell cycle to growth of the E1B mutant virus was determined by infecting HeLa cells synchronized to S phase or G_1. Compared to cells infected in G_1, cells infected in S phase with the E1B mutant virus had a greater number of infectious centers (Fig. 7 and Table 1), produced higher levels of virus progeny (Fig. 8), and demonstrated a near wild-type cytopathic effect (Fig. 9). These data demonstrate that Ad mutants that fail to express the E1B 55-kDa protein have acquired a dependence on the cell cycle for virus production.

When infected during S phase, HeLa cells support efficient replication of Ads that fail to express the E1B 55-kDa protein. It is not known whether the environment that complements the defect in virus production exists at the time of infection or develops during the course of the infection. Because cells in-

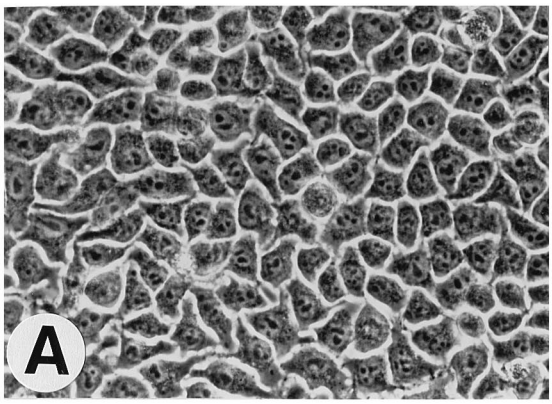
A

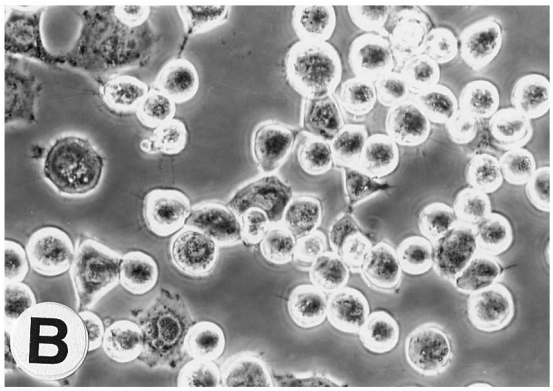
B

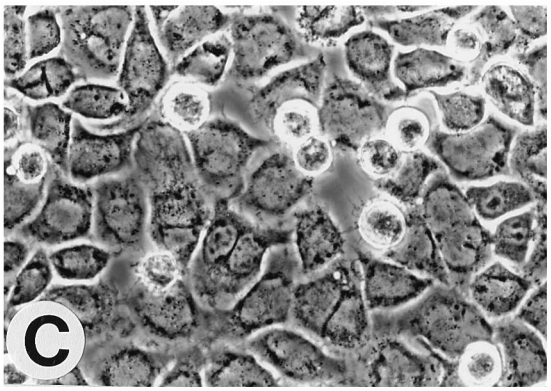
C

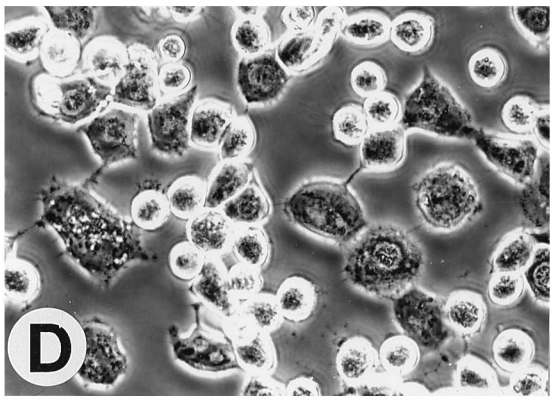
D

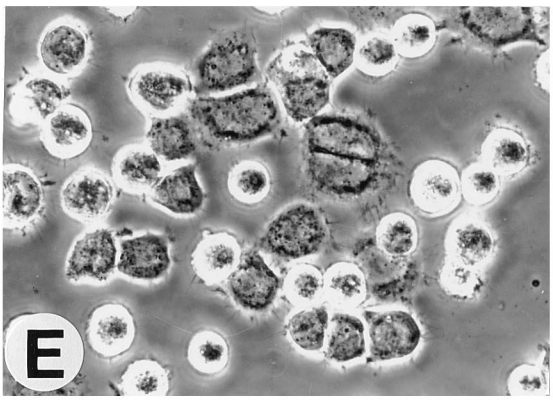
E

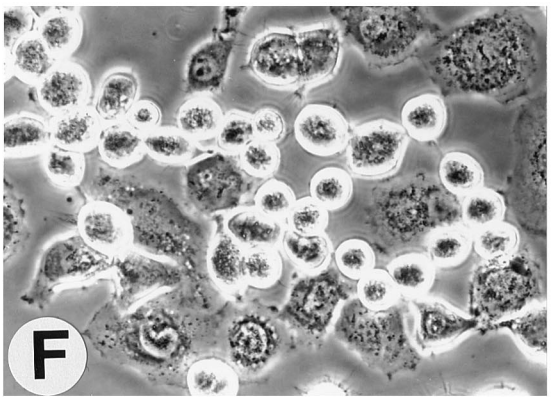
F

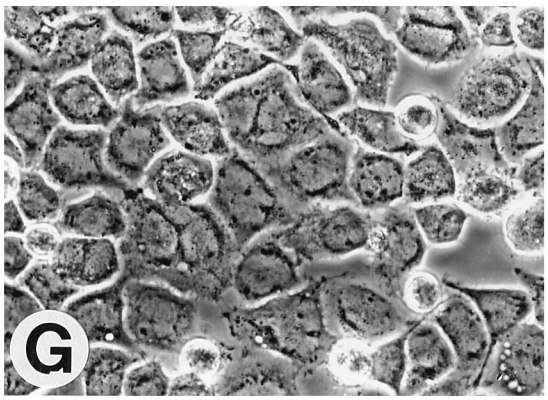
G

FIG. 9. HeLa cells infected with the E1B 55-kDa mutant virus during S phase exhibit a more severe virus-induced cytopathic effect than asynchronous cells or cells infected during G_1. Asynchronously growing HeLa cells (A to C), HeLa cells in S phase (D and E), or HeLa cells in G_1 phase (F and G) were either mock infected (A) or infected with the wild-type virus (B, D, and F) or the E1B 55-kDa mutant virus (C, E, and G) at 10 PFU per cell. At 48 h postinfection, cells were analyzed by phase-contrast microscopy. The Ad-induced cytopathic effect is characterized by cell rounding, as evidenced by the light-refractive bodies.

fected with either wild-type or E1B mutant virus fail to enter mitosis (data not shown), we favor the hypothesis that Ad infection halts normal progression of the cell cycle. Clearly the very definition of the cell cycle following infection remains uncertain. Although cells infected in S phase with the E1B mutant virus produced more virus than asynchronous or G_1 cells, they produced ninefold less virus than S phase cells infected with the wild-type virus (Fig. 8). Furthermore, by electron microscopy it appeared that each E1B 55-kDa mutant virus-infected cell containing viral particles produced fewer particles than any cell infected with the wild-type virus (compare Fig. 7A or B to C). Moreover, when applied to synchronized HeLa cells infected in S phase, both the $TCID_{50}$ assay for infectious centers (Table 1) and the plaque assay for infectious centers (data not shown) determined that between 24 to 37% of the S phase cells produced infectious E1B mutant virus; this range of values is significantly less than the 75% estimated by electron microscopy. Perhaps some of the productive cells identified by morphological means contain noninfectious particles. If so, it seems likely that the ratio of particles to PFU for virus obtained from synchronized cells infected in S phase is higher than that for virus obtained from cells infected at other stages of the cell cycle. Nonetheless, a property of S phase enables production of the E1B mutant virus although it cannot fully restore viral replication to wild-type levels.

Other viruses such as the parvoviruses, depend on S phase and the normal progression of the cell cycle for their replication. Replication of the bovine gammaherpesvirus 4 (BHV-4) DNA was shown to depend on transition through S phase. In this study, the number of cells expressing late proteins and synthesizing viral DNA among BHV-4-infected cells was inversely correlated with cell density (65). We identified only one other report of a mutant virus that acquired a dependence on the cell cycle for replication. The herpes simplex virus type 1 Vmw65 (VP16) insertion mutant was shown to depend on cells infected during S phase for early protein synthesis and replication (14). However, any relationship between the Vmw65 mutant herpesvirus and the E1B 55-kDa mutant Ad is unclear.

By contrast to synchronized cells infected with the E1B 55-kDa mutant virus, cells infected with the wild-type virus during G_1 appear slightly better suited for replication of the wild-type virus than cells infected during S phase. G_1-infected cells produced threefold more wild-type virus than S phase-infected cells. Similarly, the results in Table 1 indicate that more cells infected in G_1 produced wild-type virus than cells infected during S phase. Similar results were obtained with a plaque assay for infectious centers (data not shown). These observations suggest that infection of cells in G_1 permits the wild-type virus to more effectively establish a program of virus replication. During an Ad infection, the E1A gene products relieve growth suppression and elicit unscheduled cellular DNA synthesis by inactivating growth suppressors associated with G_1 (5, 33, 41). Therefore, it may be suggested that the E1 region of Ad is poised to promote progression from G_1 into S. When cells are infected during S phase, a cellular program of DNA synthesis has already been established, and the virus may be forced to compete with the cell for limiting factors, such as free nucleotides, that are essential for DNA and RNA synthesis. Support for this possibility can be derived from the findings of Hodge and Scharff (24) who showed that when Ad DNA synthesis began prior to initiation of cellular DNA synthesis (S phase), the subsequent initiation at the next S phase was prevented. However, when viral DNA synthesis began after the onset of cellular DNA synthesis, cellular DNA synthesis was not completely inhibited (24). Together, these findings offer an hypothesis as to why G_1 phase cells better replicate the wild-type virus than S phase cells.

In contrast to the well-established role played by the E1A proteins in deregulating the cell cycle during lytic growth, (reviewed in references 17 and 67), the E1B 55-kDa protein has not been shown to function directly in deregulating the cell cycle during virus replication. It has, however, been hypothesized that the E1B 55-kDa protein permits E1A-induced DNA synthesis by preventing p53-mediated G_1 growth arrest or apoptosis (50, 59). Such a response by p53 to viral challenge would severely hinder if not shut down the ability of the virus

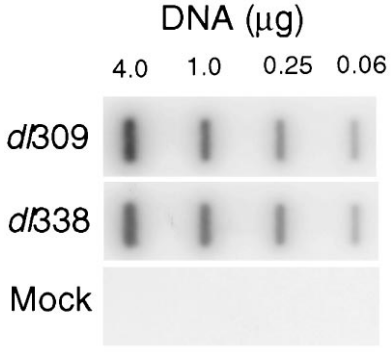

FIG. 10. E1B 55-kDa mutant virus-infected cells synthesize viral DNA at the same level as wild-type virus infection. HeLa cells were infected with either the wild-type virus, *dl*309, or the E1B 55-kDa mutant virus, *dl*338, at a multiplicity of 10 PFU per cell. Total cellular DNA was isolated from equal numbers of Ad-infected HeLa cells 20 h postinfection. Total DNA in the amount indicated above each lane was transferred to a nylon membrane, denatured, and hybridized with radioactive Ad-specific DNA probes generated by random-primed synthesis. Hybridized probe was quantified by densitometry, and mock-infected background was subtracted. Identical amounts of viral DNA were measured in E1B 55-kDa mutant virus-infected cells and wild-type virus-infected cells.

TABLE 2. Virus yield following infection of wild-type p53 and p53-null cell lines[a]

Cell line	p53 status	Virus yield (10^6 PFU per ml)[b]		
		E1B mutant	Wild type	Fold difference[c]
H460	Wild type	6.6 (4.5, 10)	120 (40, 230)	18
A549		44 (33, 58)	84 (46, 99)	1.9
H358	Null	2.9 (1.3, 4.7)	19 (7, 41)	6.4
Saos-2		1.1 (0.5, 2.2)	14 (7, 24)	13

[a] A total of 8×10^5 of the indicated cells in 4 ml were infected with 5 PFU per cell of either the wild-type virus, *dl*309, or the E1B mutant virus, *dl*338. The cells were lysed in a volume of 4 ml 2 days postinfection, and the titer of the progeny virus was determined by plaque assay with 293 cells.

[b] The virus yield was obtained by averaging the results of 6 to 10 independent measurements. The results are presented as the average (minimum/maximum).

[c] The fold difference is the ratio of wild-type virus yield to E1B mutant virus yield in the indicated cell line.

to transform cells or synthesize viral DNA and establish a lytic infection (16, 37, 69). However, replication of the E1B 55-kDa mutant virus was not related to the status of p53 in the five cell lines examined in this study (Fig. 8 and Table 2). Thus, these data suggest that the E1B 55-kDa protein relieves growth constraints of the cell cycle by mechanisms independent of p53. Other interactions between the E1B 55-kDa protein and cellular regulatory factors may exist to permit virus production in the wild-type Ad infection. Such positively acting regulatory factors may be made available or negatively acting factors may be absent when cells are infected during the S phase of the cell cycle.

Based on the known functions of the E1B 55-kDa protein in lytic infection, the inability of the E1B mutant virus to produce progeny virions in all infected cells may be linked to the defect in viral mRNA transport. The E1B 55-kDa mutant virus appears able to enter the late phase of viral replication. However, although late genes are transcribed, the transcripts never reach the cytoplasm (45). S phase cells may provide a property or factor that partially compensates for the E1B 55-kDa protein in promoting transport of viral mRNA. Work is in progress to determine if a correlation exists between the cell cycle-dependent replication and the mRNA transport defect of the E1B 55-kDa mutant virus. For example, if cell cycle-dependent viral replication and the mRNA transport defect are linked, the E4 34-kDa mutant virus may also depend on the cell cycle for virus production. As previously suggested, the E1B 55-kDa–E4 34-kDa protein complex may interact with and recruit a limiting cellular factor to the sites of viral RNA processing to aid in the transport of viral mRNA (43). Perhaps this factor is abundant in cells infected in S phase and can promote the transport of viral RNA in the absence of the E1B 55-kDa–E4 34-kDa complex. If such a factor exists, our previous work suggests that the cellular factor may be unique to primate cells (19). Several cellular proteins have been shown to function in cell cycle regulation and mRNA transport such that these two regulatory processes may be linked to some extent. For example, Ran/TC4 (31, 52, 53, 57) and the regulator of chromatin condensation-1, RCC1 (1, 12, 27, 28, 42), are cellular proteins involved in mediating both RNA transport and cell cycle progression. These or similar proteins would be potential targets of the E1B 55-kDa protein.

ACKNOWLEDGMENTS

This work was supported in part by Public Health Service grant AI35589 from the National Institute of Allergy and Infectious Disease to D.A.O. and grant CA12197 from the National Cancer Institute to the Comprehensive Cancer Center of Wake Forest University. Tissue culture reagents and services were provided by the Tissue Culture Core Laboratory of the Comprehensive Cancer Center of Wake Forest University supported in part by NIH grant CA12197.

We gratefully acknowledge Tom Shenk (Princeton University) for the *dl*309 and *dl*338 viruses, Arnie Berk (U.C.L.A.) for the *dl*1520D virus, and Arnie Levine (Princeton University) for the B6-8 hybridoma cell line. We thank Doug Lyles and Griff Parks (Wake Forest University) for critically reading the manuscript and for scientific discussions. We also thank Ken Grant and Nora Zbieranski of Wake Forest University for invaluable assistance with electron microscopy and FACS analysis, respectively.

ADDENDUM IN PROOF

After this article was accepted, Bischoff et al. (J. R. Bischoff, D. H. Kirn, A. Williams, C. Heise, S. Horn, M. Muna, L. Ng, J. A. Nye, A. Sampson-Johannes, A. Fattaey, and F. McCormick, Science **274:**373–376, 1996) reported that the E1B mutant virus *dl*1520 selectively replicates in and kills p53-deficient human tumor cells. These authors also reported that *dl*1520 fails to replicate in and kill human tumor cells expressing wild-type p53. In contrast to the findings of these investigators, we found that replication of the E1B mutant virus *dl*338 was not necessarily blocked by the presence of wild-type p53. Our findings, which include an analysis of the replication of *dl*1520 in HeLa cells, suggest that the fraction of cells in S phase at the time of viral challenge, rather than the status of p53, is prognostic for a productive infection by an E1B mutant virus. This hypothesis, if substantiated, would suggest that the range of human tumor cells that can be killed by the E1B mutant virus extends beyond p53-deficient cells.

REFERENCES

1. **Amberg, D. C., M. Fleischmann, I. Stagljar, C. N. Cole, and M. Aebi.** 1993. Nuclear PRP20 protein is required for mRNA export. EMBO J. **12:**233–241.
2. **Ausubel, F. M., R. Brent, R. E. Kingston, D. D. Moore, J. G. Seidman, J. A. Smith, and K. S. Struhl (ed.).** 1993. Current protocols in molecular biology, vol. 2. Greene Publishing Associates and John Wiley and Sons, Inc., New York, N.Y.
3. **Babich, A., L. T. Feldman, J. R. Nevins, J. E. Darnell, and C. Weinberger.** 1983. Effect of adenovirus on metabolism of specific host mRNAs: transport control and specific translational discrimination. Mol. Cell. Biol. **3:**1212–1221.
4. **Babiss, L. E., H. S. Ginsberg, and J. E. Darnell.** 1985. Adenovirus E1B proteins are required for accumulation of late viral mRNA and for effects on cellular mRNA translation and transport. Mol. Cell. Biol. **5:**2552–2558.
5. **Bagchi, S., P. Raychaudhuri, and J. R. Nevins.** 1990. Adenovirus E1A proteins can dissociate heterodimeric complexes involving the E2F transcription factor: a novel mechanism for E1A trans-activation. Cell **62:**659–669.
6. **Barker, D. D., and A. J. Berk.** 1987. Adenovirus proteins from both E1B reading frames are required for transformation of rodent cells by viral infection and DNA transfection. Virology **156:**107–121.
7. **Boulanger, P. A., and G. E. Blair.** 1991. Expression and interactions of human adenovirus oncoproteins. Biochem. J. **275:**281–299.
8. **Bridge, E., and G. Ketner.** 1990. Interaction of adenoviral E4 and E1B products in late gene expression. Virology **174:**345–353.
9. **Brigati, D. J., D. Myerson, J. J. Leary, B. Spalholz, S. Z. Travis, C. K. Y. Fong, G. D. Hsiung, and D. C. Ward.** 1983. Detection of viral genomes in cultured cells and paraffin-embedded tissue sections using biotin-labeled hybridization probes. Virology **126:**32–50.
10. **Brower, M., D. N. Carney, H. K. Oie, A. F. Gazdar, and J. D. Minna.** 1986. Growth of cell lines and clinical specimens of human non-small cell lung cancer in a serum-free defined medium. Cancer Res. **46:**798–806.
11. **Cao, G., L.-M. Liu, and S. F. Cleary.** 1991. Modified method of mammalian cell synchronization improves yield and degree of synchrony. Exp. Cell Res. **193:**405–410.
12. **Cheng, Y., J. E. Dahlberg, and E. Lund.** 1995. Diverse effects of the guanine nucleotide exchange factor RCC1 on RNA transport. Science **267:**1807–1810.
13. **Chiou, S.-K., C.-C. Tseng, L. Rao, and E. White.** 1994. Functional complementation of the adenovirus E1B 19-kilodalton protein with Bcl-2 in the inhibition of apoptosis in infected cells. J. Virol. **68:**6553–6566.
14. **Daksis, J. I., and C. M. Preston.** 1992. Herpes simplex virus immediate early gene expression in the absence of transinduction by Vmw65 varies during the cell cycle. Virology **189:**196–202.
15. **Davis, B. D., R. Dulbecco, H. N. Eisen, and H. S. Ginsberg.** 1990. Microbiology, 4th ed. J. B. Lippincott Co., Philadelphia, Pa.
16. **Debbas, M., and E. White.** 1993. Wild-type p53 mediates apoptosis by E1A, which is inhibited by E1B. Genes Dev. **7:**546–554.
17. **Dyson, N., and E. Harlow.** 1992. Adenovirus E1A targets key regulators of cell proliferation. Cancer Surv. **12:**161–195.
18. **Gallimore, P. H., P. A. Sharp, and J. Sambrook.** 1974. Viral DNA in transformed cells. II. A study of the sequences of adenovirus 2 DNA in nine lines of transformed rat cells using specific fragments of the viral genome. J. Mol. Biol. **89:**49–72.
19. **Goodrum, F. D., T. Shenk, and D. A. Ornelles.** 1996. Adenovirus early region 4 34-kilodalton protein directs the nuclear localization of the early region 1B 55-kilodalton protein in primate cells. J. Virol. **70:**6323–6335.
20. **Graham, F. L., P. J. Abrahams, C. Mulder, H. L. Heijneker, S. O. Warnaar, A. J. de Vries, W. Fiers, and A. J. van der Eb.** 1974. Studies on in vitro transformation by DNA and DNA fragments of human adenoviruses and simian virus 40. Cold Spring Harbor Symp. Quant. Biol. **39:**637–650.
21. **Graham, F. L., J. Smiley, W. C. Russell, and R. Nairn.** 1977. Characteristics of a human cell line transformed by DNA from human adenovirus type 5. J. Gen. Virol. **36:**59–72.
22. **Grand, R. J. A., M. L. Grant, and P. H. Gallimore.** 1994. Enhanced expression of p53 in human cells infected with mutant adenoviruses. Virology **203:**229–240.

23. **Halbert, D. N., J. R. Cutt, and T. Shenk.** 1985. Adenovirus early region 4 encodes functions required for efficient DNA replication, late gene expression, and host cell shutoff. J. Virol. **56:**250–257.
24. **Hodge, L. D., and M. D. Scharff.** 1969. Effect of adenovirus on host cell DNA synthesis in synchronized cells. Virology **37:**554–564.
25. **Jones, N., and T. Shenk.** 1978. Isolation of deletion and substitution mutants of adenovirus type 5. Cell **13:**181–186.
26. **Jones, N., and T. Shenk.** 1979. Isolation of Ad5 host range deletion mutants defective in transformation of rat embryo cells. Cell **17:**683–689.
27. **Kadowaki, T., D. Goldfarb, L. M. Spitz, A. M. Tartakoff, and M. Ohno.** 1993. Regulation of RNA processing and transport by a nuclear guanine release protein and members of the Ras superfamily. EMBO J. **12:**2929–2937.
28. **Kadowaki, T. D., Y. Zhao, and A. M. Tartakoff.** 1992. A conditional yeast mutant deficient in mRNA transport from nucleus to cytoplasm. Proc. Natl. Acad. Sci. USA **89:**2312–2316.
29. **Kafotos, F. C., C. W. Jones, and A. Efstratiadis.** 1979. Determination of nucleic acid sequence homologies and relative concentrations by a dot hybridization procedure. Nucleic Acids Res. **7:**1541–1552.
30. **Kao, C. C., P. R. Yew, and A. J. Berk.** 1990. Domains required for in vitro association between the cellular p53 and the adenovirus 2 E1B 55kD proteins. Virology **179:**806–814.
31. **Kornbluth, S., M. Dasso, and J. Newport.** 1994. Evidence for a dual role for TC4 protein in regulating nuclear structure and cell cycle progression. J. Cell Biol. **125:**705–719.
32. **Koza, R. A., and E. J. Herbst.** 1992. Deficiencies in DNA replication and cell cycle progression in polyamine-depleted HeLa cells. Biochem. J. **281:**87–93.
33. **La Thangue, N. B.** 1994. DP and E2F proteins: components of a heterodimeric transcription factor implicated in cell cycle control. Curr. Opin. Cell. Biol. **6:**443–450.
34. **Ledinko, N.** 1966. Changes in metabolic and enzymatic activities of monkey kidney cells after infection with adenovirus 2. Virology **28:**679–692.
35. **Lehman, T. A., W. P. Bennett, R. A. Metcalf, J. A. Welsh, J. Ecker, R. V. Modali, S. Ullrich, J. W. Romano, E. Appella, J. R. Testa, B. I. Gerwin, and C. C. Harris.** 1991. p53 mutations, ras mutations, and p53-heat shock protein complexes in human lung carcinoma cell lines. Cancer Res. **51:**4090–4096.
36. **Leppard, K. N., and T. Shenk.** 1989. The adenovirus E1B-55 kD protein influences mRNA transport via an intranuclear effect on RNA metabolism. EMBO J. **8:**2329–2336.
37. **Lowe, S. W., and H. E. Ruley.** 1993. Stabilization of the p53 tumor suppressor is induced by adenovirus 5 E1A and accompanies apoptosis. Genes Dev. **7:**535–545.
38. **Martinez-Palomo, A.** 1968. Ultrastructural study of the replication of human adenovirus type 12 in cultured cells. Pathol. Microbiol. **31:**147–164.
39. **Masuda, H., C. Miller, H. P. Koeffler, H. Battifora, and M. J. Cline.** 1987. Rearrangement of the p53 gene in human osteogenic sarcomas. Proc. Natl. Acad. Sci. USA **84:**7716–7719.
40. **Moyne, G., E. Pichard, and W. Bernhard.** 1978. Localization of simian adenovirus 7 (SA 7) transcription and replication in lytic infection. An ultracytochemical and autoradiographical study. J. Gen. Virol. **40:**77–92.
41. **Nevins, J. R.** 1992. E2F: a link between the Rb tumor suppressor protein and viral oncoproteins. Science **258:**424–429.
42. **Nishimoto, T., E. Eilen, and C. Basilico.** 1978. Premature chromatin condensation in a ts DNA-mutant of BHK cells. Cell **15:**475–483.
43. **Ornelles, D. A., and T. Shenk.** 1991. Localization of the adenovirus early region 1B 55-kilodalton protein during lytic infection: association with nuclear viral inclusions requires the early region 4 34-kilodalton protein. J. Virol. **65:**424–439.
44. **Pilder, S., J. Logan, and T. Shenk.** 1984. Deletion of the gene encoding the adenovirus 5 early region 1B 21,000-molecular-weight polypeptide leads to degradation of viral and host cell DNA. J. Virol. **52:**664–671.
45. **Pilder, S., M. Moore, J. Logan, and T. Shenk.** 1986. The adenovirus E1B-55K transforming polypeptide modulates transport or cytoplasmic stabilization of viral and host cell mRNAs. Mol. Cell. Biol. **6:**470–476.
46. **Puvion-Dutilleul, F., J.-P. Bachellerie, N. Visa, and E. Puvion.** 1994. Rearrangements of intranuclear structures involved in RNA processing in response to adenovirus infection. J. Cell Sci. **107:**1457–1468.
47. **Puvion-Dutilleul, F., and E. Puvion.** 1990. Analysis by in situ hybridization and autoradiography of sites of replication and storage of single- and double-stranded adenovirus type 5 DNA in lytically infected HeLa cells. J. Struct. Biol. **103:**280–289.
48. **Puvion-Dutilleul, F., and E. Puvion.** 1990. Replicating single-stranded adenovirus type 5 DNA molecules accumulate within well-defined intranuclear areas of lytically infected HeLa cells. Eur. J. Cell Biol. **52:**379–388.
49. **Puvion-Dutilleul, F., R. Roussev, and E. Puvion.** 1992. Distribution of viral RNA molecules during the adenovirus type 5 infectious cycle in HeLa cells. J. Struct. Biol. **108:**209–220.
50. **Quinlan, M. P.** 1994. Enhanced proliferation, growth factor induction and immortalization by adenovirus E1A 12S in the absence of E1B. Oncogene **9:**2639–2647.
51. **Reich, N. C., P. Sarnow, E. Duprey, and A. J. Levine.** 1983. Monoclonal antibodies which recognize native and denatured forms of the adenovirus DNA-binding protein. Virology **128:**480–484.
52. **Ren, M., E. Coutavas, P. D'Eustachio, and M. G. Rush.** 1994. Effects of mutant Ran/TC4 proteins on cell cycle progression. Mol. Cell. Biol. **14:**4216–4224.
53. **Ren, M., G. Drivas, P. D'Eustachio, and M. G. Rush.** 1993. Ran/TC4: a small nuclear GTP-binding protein that regulates DNA synthesis. J. Cell Biol. **120:**313–323.
54. **Ruley, H. E.** 1983. Adenovirus early region 1A enables viral and cellular transforming genes to transform primary cells in culture. Nature (London) **304:**602–606.
55. **Sarnow, P., C. A. Sullivan, and A. J. Levine.** 1982. A monoclonal antibody detecting the adenovirus type 5 E1b-58kD tumor antigen: characterization of the E1b-58kD tumor antigen in adenovirus-infected and -transformed cells. Virology **120:**510–517.
56. **Scheffner, M., B. A. Werness, J. M. Huibregtse, A. J. Levine, and P. M. Howley.** 1990. The E6 oncoprotein encoded by human papillomavirus types 16 and 18 promotes the degradation of p53. Cell **63:**1129–1136.
57. **Schlenstedt, G., C. Saaverda, D. J. Loeb, C. N. Cole, and P. A. Silver.** 1995. The GTP-bound form of the yeast Ran/TC4 homologue blocks nuclear protein import and the appearance of poly (A)+ RNA in the cytoplasm. Proc. Natl. Acad. Sci. USA **92:**225–229.
58. **Schmidt, M. R., and R. T. Woodland.** 1990. Virus-lymphocyte interactions: inductive signals necessary to render B lymphocytes susceptible to vesicular stomatitis virus infection. J. Virol. **64:**3289–3296.
59. **Shepherd, S. E., J. A. Howe, J. S. Mymryk, and S. T. Bayley.** 1993. Induction of the cell cycle in baby rat kidney cells by adenovirus type 5 E1A in the absence of E1B and a possible influence of p53. J. Virol. **67:**2944–2949.
60. **Spitkovsky, D., P. Steiner, R. V. Gopalkrishnan, M. Eilers, and P. Jansen-Durr.** 1995. The role of p53 in coordinated regulation of cyclin D1 and p21 gene expression by the adenovirus E1A and E1B oncogenes. Oncogene **10:**2421–2425.
61. **Stillman, B.** 1986. Functions of the adenovirus E1B tumor antigens. Cancer Surv. **5:**389–404.
62. **Takahashi, T., M. M. Nau, I. Chiba, M. J. Birrer, R. K. Rosenberg, M. Vinocour, M. Levitt, H. Pass, A. F. Gazdar, and J. D. Minna.** 1989. p53: a frequent target for genetic abnormalities in lung cancer. Science **246:**491–494.
63. **Urbani, L., S. W. Sherwood, and R. T. Schimke.** 1995. Dissociation of nuclear and cytoplasmic cell cycle progression by drugs employed in cell synchronization. Exp. Cell Res. **219:**159–168.
64. **van den Elsen, P. J., A. Houweling, and A. J. van der Eb.** 1983. Morphological transformation of human adenoviruses is determined to a large extent by gene products of region E1A. Virology **131:**242–246.
65. **Vanderplasschen, A., M. Goltz, J. Lyaku, C. Benarafa, H.-J. Buhk, E. Thiry, and P.-P. Pastoret.** 1995. The replication in vitro of the gammaherpesvirus bovine herpesvirus 4 is restricted by its DNA synthesis dependence on the S phase of the cell cycle. Virology **213:**328–340.
66. **Voelkerding, K., and D. F. Klessig.** 1986. Identification of two nuclear subclasses of the adenovirus type 5-encoded DNA binding protein. J. Virol. **60:**353–362.
67. **Vousden, K. H.** 1995. Regulation of the cell cycle by viral oncoproteins. Semin. Cancer Biol. **6:**109–116.
68. **Werness, B. A., A. J. Levine, and P. M. Howley.** 1990. Association of human papilloma virus types 16 and 18 E6 proteins with p53. Science **248:**76–79.
69. **White, E.** 1994. Function of the adenovirus E1B oncogene in infected and transformed cells. Semin. Virol. **5:**341–348.
70. **Wolgemuth, D. J., and M.-T. Hsu.** 1981. Visualization of nascent RNA transcripts and simultaneous transcription and replication in viral nucleoprotein complexes from adenovirus 2-infected HeLa cells. J. Mol. Biol. **147:**247–268.
71. **Yamaguchi, H., K. Hosokawa, Z.-L. Jiang, A. Takahashi, T. Ikehara, and H. Miyamoto.** 1993. Arrest of cell cycle progression in HeLa cells in the early G1 phase in K+-depleted conditions and its recovery upon addition of insulin and LDL. J. Cell. Biochem. **53:**13–20.
72. **Yew, P. R., and A. J. Berk.** 1992. Inhibition of p53 transactivation required for transformation by adenovirus early 1B protein. Nature (London) **357:**82.
73. **Yew, R. P., X. Lui, and A. J. Berk.** 1994. Adenovirus E1B oncoprotein tethers a transcriptional repression domain to p53. Genes Dev. **8:**190–202.
74. **Zantema, A., J. A. M. Fransen, A. Davis-Oliver, F. C. S. Ramaekers, G. P. Vooijs, B. DeLeys, and A. J. van der Eb.** 1985. Localization of the E1B proteins of adenovirus type 5 in transformed cells as revealed by interaction with monoclonal antibodies. Virology **142:**44–58.
75. **Zantema, A., P. I. Schrier, A. Davis-Oliver, T. van Laar, R. T. M. J. Vaessen, and A. J. van der Eb.** 1985. Adenovirus serotype determines association and localization of the large E1B tumor antigen and cellular tumor antigen p53 in transformed cells. Mol. Cell. Biol. **5:**3084–3091.